This article has been accepted for publication in a future issue of this journal, but has not been fully edited. Content may change prior to final publication. Citation information: DOI 10.1109/JSEN.2019.2934943, IEEE Sensors Journal

Evaluation of printed P(VDF-TrFE) pressure sensor signal quality in arterial pulse wave measurement

Mika-Matti Laurila, Mikko Peltokangas, Karem Lozano Montero, Tuomo Siponkoski, Jari Juuti, Sampo Tuukkanen, Niku Oksala, Antti Vehkaoja*, *Member, IEEE*, and Matti Mäntysalo*

***Abstract*— In this contribution, we evaluate the performance of an additively fabricated piezoelectric poly(vinylidenefluoride-co-trifluoroethylene) (P(VDF-TrFE)) based dynamic pressure sensor in non-invasive arterial pulse wave (PW) measurement. Additively fabricated piezoelectric sensors have high potential for the realization of affordable and unobtrusive PW measurement systems which could enable the long-term monitoring of patients with cardiovascular diseases (CVDs). However, the accuracy and reliability of such sensors have not been extensively studied before. We propose an additive fabrication process for a P(VDF-TrFE) PW-sensor, measure PW from the radial artery at the wrist from 22 healthy volunteer subjects, calculate clinically relevant parameters based on the PW waveform and compare their values to the values obtained from concurrent measurement with an electromechanical film (EMFi) based reference sensor, used earlier in several clinical studies. We show that the signals recorded with the two sensors, as well as the radial augmentation index (rAIx) and the stiffness index (SI) calculated from them, are in good agreement with each other. These results demonstrate that the additively fabricated P(VDF-TrFE) PW sensors can reach a suitable level of accuracy and reliability for clinical use.**

***Index Terms*—Printed electronics, pulse wave measurement, radial artery, piezoelectric dynamic pressure sensor, P(VDF-TrFE), electret material, EMFi**

I. Introduction

NON-INVASIVE measurement of arterial pulse wave (PW) has emerged as a potential candidate for estimating the arterial stiffness which is considered an indicator of several cardiovascular diseases (CVD) and its manifestations such as coronary artery disease (especially acute myocardial infarction), cerebrovascular disease (especially ischemic stroke), hypertension and heart failure [1][2]. CVDs in general are among the most common causes of death in the world [3] and their prevention at different stages, treatment, and follow-up cause significant costs. Long-term monitoring enabled by non-invasive measurement methods offers a potential solution for this problem because high-risk individuals may be monitored regularly or even during their daily routines and referred to further examinations and timely treatment when abnormal changes in physiological signals are observed. It would also enable a continuous follow up for patients who have undergone a recent treatment for CVD.

The large-scale screening and continuous monitoring of the whole risk population sets requirements for a PW measurement device, which should be comfortable to use (i.e. unobtrusive), affordable, accurate, and reliable. The current non-invasive PW measurement devices (such as [4]) cannot meet these criteria, because of their large physical size, cost, and need for a professional operator for the measurement. So far, the requirement of unobtrusiveness has been met with several different types of thin and ultra-thin PW pressure sensors based on piezoresistive [5], piezoelectric [6] and capacitive measurement principles [7]. Also, the affordability requirement has been solved by employing solution processed materials and additive fabrication technologies such as inkjet [8], screen [11], and gravure printing [12] or spin coating [13] and impregnation [14]. As an additional benefit, the use of additive fabrication technologies enables fabrication of conformable health patches and temporary tattoos [15][16] which have been previously demonstrated for measuring other vital signs such as ECG [17], pulse oximetry [18], and temperature [19]. In the future, additive fabrication technologies could also enable the integration of the whole measurement system on a single foil in cost effective manner [20] thereby allowing the patient to use the device without the need for professional help. However, *the accuracy and reliability* of the proposed PW sensors have not been usually validated with a sufficient number of subjects, or by using a reference device for the measurement. For example in references [5]-[14], the number of subjects is either one, or not indicated at all. Furthermore, none of the aforementioned studies compare the measured pulse wave signals to concurrent

Manuscript submitted xx.xx.2019. This work was supported by Academy of Finland under Grant #310617, #310618, and #320019. M. Mäntysalo is supported by Academy of Finland Grants #288945 and #319408. A. Vehkaoja is supported by Academy of Finland Grant #292477.

M.-M. Laurila and M. Peltokangas contributed equally to this work.

*A. Vehkaoja and M. Mäntysalo share the senior-authorship.

M.-M. Laurila, K. L. Montero, and M. Mäntysalo are with the Faculty of Information Technology and Communication Sciences, Tampere University, Korkeakoulunkatu 3, 33720, Tampere, Finland. M.-M. Laurila is the corresponding author (e-mail: mika-matti.laurila@tuni.fi). M. Peltokangas, S. Tuukkanen, N. Oksala, and A. Vehkaoja are with the Faculty of Medicine and Health Technology, Tampere University, Tampere, Finland. T. Siponkoski and J. Juuti are with the Microelectronics Research Unit, Oulu University, Oulu, Finland.

This article has been accepted for publication in a future issue of this journal, but has not been fully edited. Content may change prior to final publication. Citation information: DOI 10.1109/JSEN.2019.2934943, IEEE Sensors Journal

measurement with a validated PW sensor. In most cases, the parameters calculated based by the PW signals are compared to literature values based on the patients' gender, age and health (e.g. [6], [8]-[14]).

Especially the piezoelectric polymer poly(vinylidene-fluoride-co-trifluoroethylene) (P(VDF-TrFE)) has high potential for meeting the aforementioned requirements due to its solution processability, which enables affordable fabrication with additive printing methods, and ability to form thin films for unobtrusive user-experience [9][10][11]. In this contribution, we study *the accuracy and reliability* of additively fabricated piezoelectric P(VDF-TrFE) PW sensor signal quality by comparing it to a PW signal obtained concurrently with a reference sensor made of electromechanical film (EMFi) electret material, which has been used earlier in several clinical studies for collecting PW data [21][22]. Furthermore, 22 test subjects are examined which enables statistical comparison between the proposed P(VDF-TrFE) sensor and the reference sensor. The aim is to demonstrate that additively fabricated P(VDF-TrFE) PW sensors can reach a suitable level of *accuracy and reliability* for clinical use.

II. Materials and Methods

A. PW sensor fabrication process

The structure of the P(VDF-TrFE) PW sensor is shown in Fig. 1a. and a scanning electron microscope (SEM) image of the sensor cross-section is shown in Fig. 1b. Polyethyleneterephalate (PET) substrates (Melinex ST506, DuPont) with a thickness of 125 µm were rinsed in isopropyl alcohol. A circular bottom electrode 15 mm in diameter was printed with an inkjet printer (DMP-2801, Fujifilm Dimatix) using Ag-nanoparticle ink (DGP 40LT-15C, Advanced Nanoproducts) and the following printing parameters: 30 µm drop spacing and 45 °C stage temperature. The electrode was sintered in a convection oven at 150 °C for 1 hour. The P(VDF-TrFE) ink (Ink P, Piezotech Arkema Group) was applied on the bottom electrode using an automatic bar coater (Motorized Film Applicator CX4, MTV Messtechnik) with a wet thickness of approximately 200 µm. The P(VDF-TrFE) was cured in a convection oven in 135 °C for 1 hour followed by slow cool down to room temperature (the oven was turned off and samples left inside until they reached room temperature). Circular top electrode 15 mm in diameter was screen-printed using PEDOT:PSS ink (Clevios S V4 STAB, Heraeus) and a semi-automatic screen printer (TIC SCF-300, Eickmeyer). The squeegee angle was set to 90° while the squeegee speed and snap off distance were adjusted manually. The screen was a thermotropic liquid crystal polymer screen (V Screen Next, NBC Meshtec) with a 20 µm thread and a 40 µm opening width. The PEDOT:PSS ink was cured in 100 °C for 1 hour followed by slow cool-down to room temperature. The samples were poled in a non-stressed state at room temperature using a poling field with a continuously increasing sinusoidal waveform of 50 mHz frequency, zero offset, and maximum amplitude of 700 kV/cm as shown in Fig. 2. The entire 300-second poling cycle was applied three times in a row for each sensor. The poling field was generated by an arbitrary waveform generator (33500B, Keysight) connected to a high voltage AC-amplifier (610C, TREK) and monitored by oscilloscope (DSOX2002A, Keysight). An approximately 2 µm thick Parylene C (GALXYL C, Galentis) layer was applied on top of the sensor using chemical vapor deposition (LabTop 3000, Para Tech Coating) in order to form a hermetic seal to prevent the degradation of the top electrode.

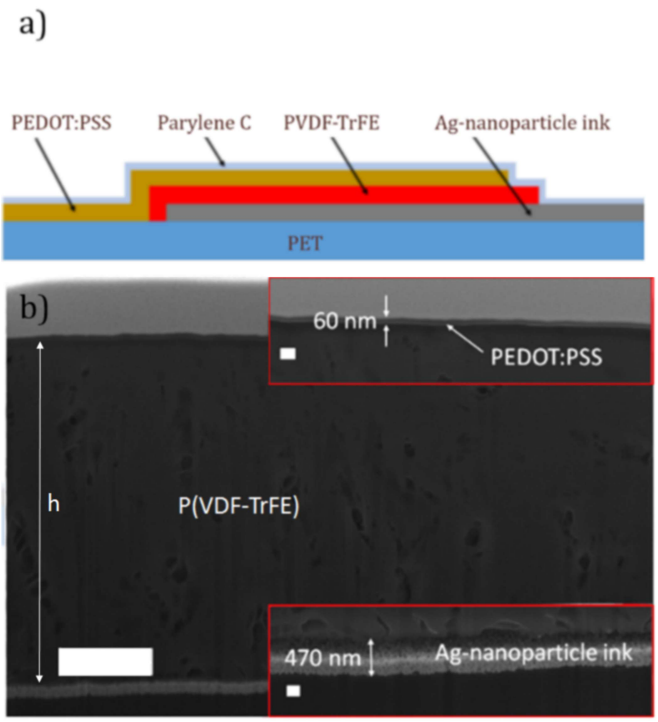

Fig. 1. Structure of the P(VDF-TrFE) PW-sensor (a) and SEM image of the FIB cross-section of the P(VDF-TrFE) PW-sensor (b). The scale bars in (b) are 2 µm (main image) and 200 nm (inserts).

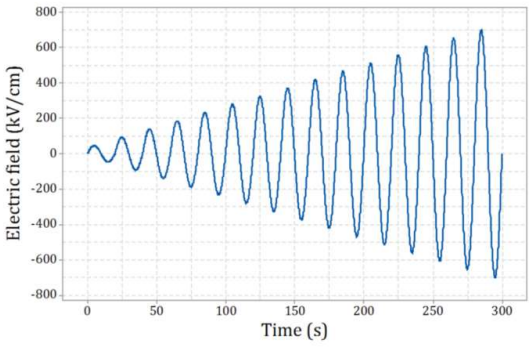

Fig. 2. Poling field used in P(VDF-TrFE) sensor fabrication.

B. Crosscut sample preparation

A crosscut sample of the PW sensor was prepared and the morphology of the sample studied using focused ion beam for cutting scanning electron microscope for studying the

This article has been accepted for publication in a future issue of this journal, but has not been fully edited. Content may change prior to final publication. Citation information: DOI 10.1109/JSEN.2019.2934943, IEEE Sensors Journal

morphology (FIBSEM, Crossbeam 540, Zeiss, Germany). The cross-section was prepared by depositing a Pt protection layer on the region of interest and by using Ga ions to mill the cross-section under the Pt covering layer. Prior to FIBSEM studies, the sensors were carbon-coated to avoid sample charging during the milling process.

Sample cross-sections for more comprehensive thickness measurements were prepared by mounting samples in epoxy and grinding/polishing the samples to a suitable observation depth using an automatic grinding/polishing tool (RotoPol-21, Struers). An optical microscope (BX51, Olympus) with 100X objective was used to study the cross-sections.

C. *Piezoelectric and electrical characterization*

The ferroelectric polarization versus electric field (PE) hysteresis loops were measured using a ferroelectric material tester (LC Precision, Radiant Technologies, USA) connected to a 10 kV high voltage amplifier (Precision 10kV, HVI-SC). The progression of the PE-loop was measured at electric fields of 400, 500, 600 and 700 kV/cm and the saturated PE-loops at 750 kV/cm. The measurement frequency was 2.5 Hz in all cases.

The performance of piezoelectric materials is described by the piezoelectric d_{xy}-coefficient matrix, which relates the mechanical stress to the electric field generated across the material, and in which the subscript *x* is related to the direction of mechanical stress and subscript *y* to the dipole direction [23]. For example, the d_{33}-coefficient refers to the case where the stress is in the parallel direction to the molecular dipoles generated during the poling process (i.e. direction of the poling field). In the case of parallel plate capacitor type sensor structures, such as the proposed P(VDF-TrFE) PW sensor, this direction is orthogonal to the electrode surface. On the other hand, charge generation due to transverse or shear stresses are described by the piezoelectric coefficients d_{31} and d_{32}. However, the characterization of these bulk material properties is challenging for thin film piezoelectric layers fabricated on flexible substrates and sandwiched between electrodes, because the deformation of additional material layers will affect the measurement. For this reason, the effective piezoelectric coefficients are often used instead of the aforementioned bulk material coefficients. For example, the effective piezoelectric coefficient $d_{33.f}$ is defined as

$$d_{33.f} = d_{33} - 2d_{31}\frac{s_{13}^E}{s_{11}^E + s_{12}^E} \quad (1)$$

where s_{xy}^E is the elastic compliance constant in *xy*-direction at constant electric field *E* [24].

The effective piezoelectric coefficient $d_{33.f}$ of the printed P(VDF-TrFE) and EMFi PW-sensors were determined using an in-house built Berlincourt setup described in [23]. In this setup, the $d_{33.f}$ describes the charge generation in the area where the stress is orthogonal to the electrode surface i.e. directly underneath the force sensor probe head (Fig. 3a, area A). However, the area adjacent to the force sensor probe head may also have a small contribution to the total amount of generated charges because it is also covered with electrodes (Fig 3a, area B). In this area, the loading is multi-directional and the charge generation may be affected by other d_{xy}-coefficients as well and depending on the dominating force component, the $d_{33.f}$ may be either amplified or attenuated. The $d_{33.f}$ measurement setup is composed of an electrodynamic actuator (Mini-Shaker Type 4810, Brüel & Kjaer) generating the mechanical excitation on a sensor, as well as dynamic (209C02, PCB Piezotronics) and static force sensors (ELFS-T3E-20L Measurement Specialties Inc.), and a charge amplifier to determine the generated amount of charge. A static force of 3 N was used to clamp a circular force probe with 4 mm diameter to the sensor. A sinusoidal dynamic normal force of 1 N with a frequency of 5 Hz was applied to the probe while simultaneously measuring the generated charge. A Matlab based script was used to fit sinusoidals on the dynamic force output signal and charge output signals and the sensitivity was calculated by dividing the amplitudes of these signals. Each sensor was measured from five points as shown in Fig. 3b and the average value of these measurements was used to indicate the $d_{33.f}$ value for the sensor.

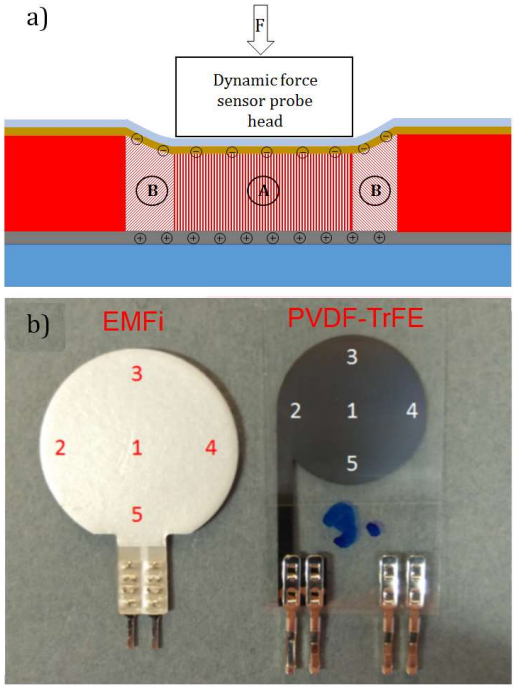

Fig. 3. (a) Schematic of effective piezoelectric $d_{33.f}$ measurement; explanation for the areas A and B are given in the main text. (b) EMFi and P(VDF-TrFE) PW-sensors where the numbers indicate sensitivity measurement excitation points (b).

The capacitance of the sensors was measured with a semiconductor parameter analyzer (B1500A, Keysight) using a frequency of 1 kHz and a voltage of 2 V.

D. *Pulse wave measurement*

Radial artery PWs at the distal antebrachium in the wrist were recorded from 22 healthy volunteer test subjects (Table 1). The

This article has been accepted for publication in a future issue of this journal, but has not been fully edited. Content may change prior to final publication. Citation information: DOI 10.1109/JSEN.2019.2934943, IEEE Sensors Journal

PW signals were recorded concomitantly with the proposed P(VDF-TrFE) sensor and a commercial force sensor (EMFit S-series, EMFit Oy, Finland) made of electret material called EMFi (ElectroMechanical Film) to compare the sensor signals with each other. The measurements were conducted in supine position. The test subjects received both written and oral information on the purpose of the study, signed an informed consent, and had the chance to interrupt the study at any point without providing any reasons. The experiments were a part of the pre-clinical measurements of a study having a favorable statement from the regional ethical review board of Tampere University Hospital (R17129).

TABLE 1
DESCRIPTION OF THE STUDY SAMPLE.

Parameter	Value [median (inter-quartile range)]
Males/Females	10/12
Systolic blood pressure (mmHg)	128 (117-133)
Diastolic blood pressure (mmHg)	79 (75-83)
Mass (kg)	70 (62-78)
Height (cm)	174 (166-181)
Body-mass index (kg/m^2)	22.8 (21.3-24.8)
Age (years)	29 (25-33)

The measurement setup consisted of a custom-made wireless body sensor network (WBSN) intended originally for EMFi sensor recordings [25]. In this study, a two-channel sensor node of the WBSN contained interface circuits for a sensor stack consisting of a superimposed EMFi sensor and P(VDF-TrFE) sensor. The interface circuit includes a non-inverting voltage amplifier as a pre-amplifier and a second voltage amplifier stage with high- and low-pass filters before the analog to digital conversion. The pass-band of the second amplifier stage was limited to high-pass of 50 mHz and low-pass of 100 Hz with first and second order passive filters, respectively, and the signals were digitized with a 16-bit analogue-to-digital converter at a sampling frequency of 250 Hz.

Using a voltage pre-amplifier with piezoelectric sensors instead of a charge amplifier makes the measurement sensitivity and the high-pass cut-off frequency dependent on the capacitance of the sensor. In the initial tests, the high-pass cut-off frequency of the P(VDF-TrFE) sensor was observed to be higher than the high-pass cut-off frequency of the EMFi sensor. The capacitance and resistance of P(VDF-TrFE) sensor were measured 1.5 nF and 3.7 GΩ, respectively. In combination with 10 GΩ input resistance of the pre-amplifier, this produces a high-pass cut-off frequency of approximately 40 mHz. To confirm that the responses of the two sensors were similar, an 8.2 nF capacitor was connected in parallel with the P(VDF-TrFE) sensor in order to decrease its lower cut-off frequency to approximately 6 mHz. After this modification, the measurement pass-band was mainly determined by the filters of the second voltage amplifier stage. As a drawback, this decreased the sensitivity of the P(VDF-TrFE) sensor by a factor of 5.2.

In order to record the same PW signal concomitantly with the two sensors, the EMFi sensor was placed under the P(VDF-TrFE) sensor (Fig. 4). To improve the mechanical coupling from the superficial radial artery to the sensor stack, an ellipsoidal connection block made of plastic was attached on the P(VDF-TrFE) sensor. The combination of the sensor stack and the connection block was fixed on the rigid housing of the pre-amplifier electronics, which was tightened around the wrist using an elastic textile wrist band as shown in Fig. 4.

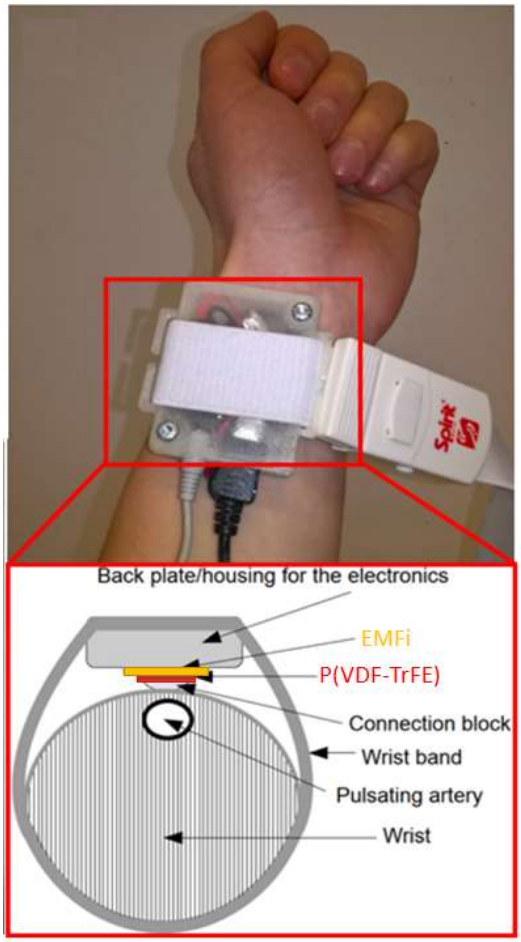

Fig. 4. Photograph and schematic of the wrist band PW-measurement setup.

E. Pulse wave analysis

Individual PW curves were extracted, low-pass filtered, and amplitude-normalized as described in an earlier study [22]. In order to improve the SNR in signal comparison, a period of seven good-quality PW curves was selected from the end of recording and averaged. The averaging-based approach is also utilized in commercial PW analyzers. The resulting averaged pulse wave was smoothed using Savitzky-Golay smoothing filter with a polynomial order of two and a window length of seven samples.

Four test subjects were excluded from further analysis as a result of too low amplitude and thus too low signal-to-noise ratio (SNR) in the P(VDF-TrFE) signal. The exclusion criteria

This article has been accepted for publication in a future issue of this journal, but has not been fully edited. Content may change prior to final publication. Citation information: DOI 10.1109/JSEN.2019.2934943, IEEE Sensors Journal

were 1) the average amplitude of P(VDF-TrFE) signal being less than the 33.3% percentile of all average P(VDF-TrFE) signal amplitudes, and 2) the ratio of the average EMFi signal amplitude and the average P(VDF-TrFE) signal amplitude being larger than the 66.7 % percentile of of all EMFi- P(VDF-TrFE) amplitude ratios. The first criterion evaluates the absolute amplitude of the P(VDF-TrFE) signal and the second criterion evaluates the amplitude of P(VDF-TrFE) signal to the reference, i.e. the assumed maximum achievable amplitude with the mechanical coupling of each experiment. The PW-derived features are computed also for these excluded test subjects and shown in the results, but they are not taken in the account in the final results.

The outputs of the different sensors were compared by extracting the fiducial points for early (P_1) and late (P_2) systolic waves as well as the diastolic wave B from the averaged PW as shown in Fig. 5 and described in [22]. Radial augmentation index (rAIx) [26] reflection index (RI) [27] and stiffness index (SI) [27] were calculated for the averaged PW curves for each test subject and each signal based on the extracted fiducial points. The rAIx is intended for the analysis of radial pressure PWs and defined as rAIx = P_2 / P_1 [26], whereas RI and SI are originally proposed for the analysis of volume PWs recorded from the index finger. The RI is defined as RI = B / P_1 and SI = h/t_{pp} in which t_{pp} is the time delay between the systolic maximum max(P_1, P_2) and diastolic maximum B (Fig. 5) and h is the test subject's height [27].

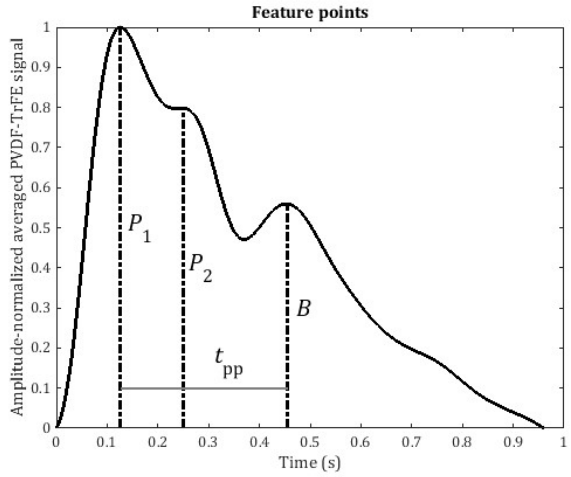

Fig. 5. An example of the feature points utilized in the sensor signal comparison.

The agreement between the aforementioned PW parameters calculated from the averaged PW curves were compared by analyzing the Bland-Altman (BA) plot [28][29][30], Pearson's correlation, and concordance correlation [31]. The BA-plot was quantitatively analyzed by computing a BA-ratio as a half-range of the limits of agreement normalized by the average of the averages of pair-wise results from different sensors [29][30]. The agreement between the methods is considered good if the BA-ratio is smaller than 0.1, moderate if the BA-ratio is between 0.1 and 0.2, and insufficient for clinical purposes if the BA-ratio is larger than 0.2 [29][30].

III. Results and Discussion

A. P(VDF-TrFE) PW-sensor

As a polycrystalline ferroelectric polymer, the P(VDF-TrFE) displays reversible polarization induced by switching of the domain structure when the electric field exceeds the coercive field E_c [34]. A polarization-electric field hysteresis loops plotted in Fig. 6a shows the progression of the polarization of a pre-poled sample (maximum poling field 700 kV/cm at room temperature) as the electric field is increased from 300 kV/cm to 700 kV/cm. When the electric field is lower than the maximum poling field, it is not possible to reorient the domain structure and only a small amount of polarization can be detected. At 700 kV/cm the electric field exceeds the maximum poling field leading to a higher polarization value. The saturated PE-loops for three pre-poled samples measured at 750 kV/cm are shown in Fig. 6b. The measured remanent polarization P_R (i.e. polarization at zero electric field) of 7.3 μC/cm^2 compares well with the datasheet value of 7.0 μC/cm^2 [35]. Also, the E_c of 505 kV/cm compares well with literature values of 500 to 600 kV/cm [36]. The high symmetry of the saturated PE-loops is noteworthy because it indicates the lack of charged defects [37] and that the asymmetric top/bottom electrodes (Ag vs. PEDOT:PSS) do not cause field direction dependent switching behavior [38]. The non-zero remanent polarization leads to the piezoelectric behavior of the P(VDF-TrFE), whereby a mechanical deformation of the material changes its internal electrical field and causes a charge accumulation on the material surfaces. This effect can be utilized in the measurement of dynamic pressure because the amount of generated charge is proportional to the change in applied pressure [34].

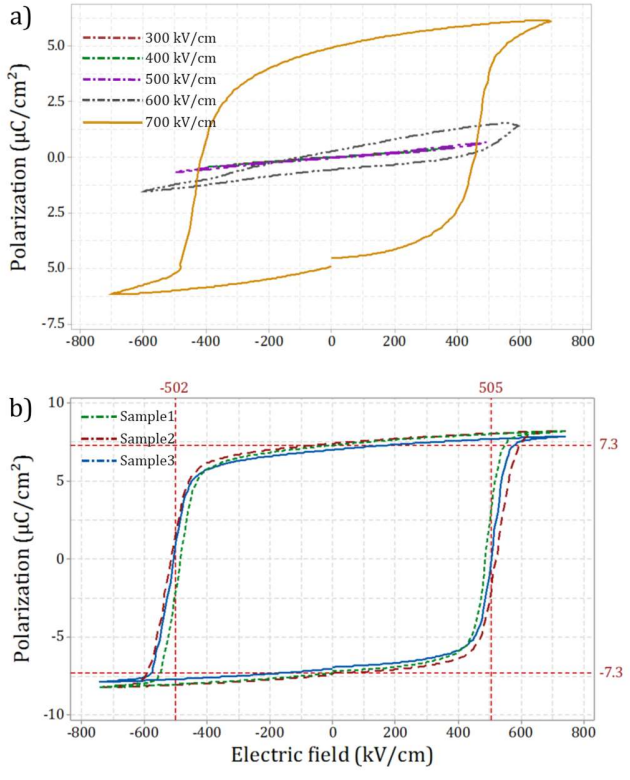

This article has been accepted for publication in a future issue of this journal, but has not been fully edited. Content may change prior to final publication. Citation information: DOI 10.1109/JSEN.2019.2934943, IEEE Sensors Journal

Fig. 6. Progression of the PE-loop for P(VDF-TrFE) sample pre-polarized at 700 kV/cm (orange: E_{max} = 300 kV; green: E_{max} = 400 kV; purple: E_{max} = 500 kV; grey: E_{max} = 600 kV; yellow: E_{max} = 700 kV) (a) and saturated hysteresis loops for three P(VDF-TrFE) samples (b). The reference lines in (b) show the average negative/positive coercive field (x-axis) and negative/positive remanent polarization (y-axis).

Uniform thickness of the P(VDF-TrFE) layer is critical for achieving homogenous sensitivity across the whole area of the sample, because the thickness will affect the electric field strength during the poling step that determines the sensitivity of the sensor [39]. Fig. 7a shows a boxplot of the thickness of the P(VDF-TrFE) layers for eight samples. The measurements were done from nine positions along the axis defined by the excitation points 2-1-4 (see Fig. 3b). The mean thickness of the samples was 9.5 ± 0.8 µm (see h in Fig. 1b), which indicates very homogenous P(VDF-TrFE) layer thickness. Sensor-to-sensor variation in $d_{33.f}$ (section II C.) was estimated from 10 samples and the results were plotted in Fig. 7b. The measured sensitivity values show a somewhat higher coefficient of variation (CV) of 10.8% compared to the CV of 5.3% for the thickness. This difference could be related to mechanical non-idealities in the sensitivity measurement setup or bending of the sample during the measurement [39]. However, the average $d_{33.f}$ piezoelectric sensitivity value for the 10 samples was (-26.9 ± 2.9) pC/N, which is very close to the literature value for piezoelectric constant d_{33} of -25 pC/N for P(VDF-TrFE) [35]. Important material properties for P(VDF-TrFE) and EMFi are summarized in Table 2.

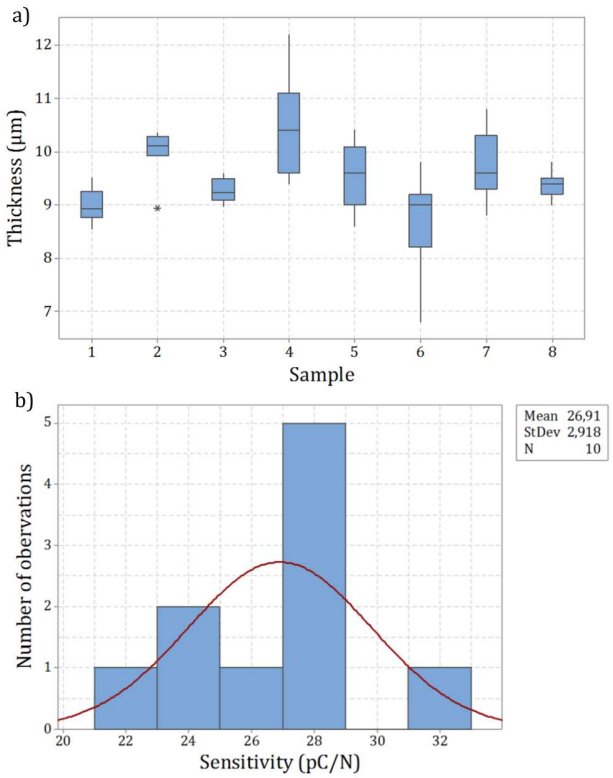

Fig. 7. Boxplot of P(VDF-TrFE*)* sensor sample thicknesses for eight samples (a) and the average longitudinal sensitivities of ten samples (b).

TABLE 2
P(VDF-TRFE) AND EMFI MATERIAL/SENSOR PROPERTIES: EFFECTIVE PIEZOELECTRIC COEFFICIENT $d_{33.f}$, REMANENT POLARIZATION P_R,COERCIVE FIELD E_C, CAPACITANCE C, AREA SPECIFIC CAPACITANCE C_{area}. P(VDF-TRFE) $d_{33.f}$ AND C ARE THE AVERAGE OF 10 SENSORS AND P_R AND E_C ARE THE AVERAGE OF 3 SENSORS. EMFI VALUES ARE BASED ON MEASUREMENT OF ONE SENSOR.

Property	P(VDF-TrFE)	EMFi
$d_{33.f}$	(-26.9 ± 2.9) pC/N	47.0 pC/N
P_R	7.3 µC/cm²	-
$-P_R$	-7.3 µC/cm²	-
E_C	505 kV/cm	-
$-E_C$	-502 kV/cm	-
C	(1.57 ± 0.067) nF	39.3 pF
C_{area}	0.44 nF/cm²	5.2 pF/cm²

B. *Pulse wave comparison*

An example of PW signals recorded from the radial artery with the two sensors is shown in Fig. 8 (EMFi: orange dotted line; P(VDF-TrFE): blue continuous line) and examples of amplitude-normalized averaged pulse waves from nine test subjects are presented in Fig. 9 (P(VDF-TrFE): orange dotted line; EMFi: blue continuous line). The signals in Fig. 8 are scaled to have similar amplitudes. With some of the test subjects, the differences in the waveforms of the EMFi and P(VDF-TrFE) sensor signals were larger than in other ones (see d) and i) in Fig. 9). In such cases, the amplitudes of P_2 and B with respect to P_1 were smaller in the P(VDF-TrFE) signals than in case of EMFi signal, which has an effect on the calculated PW parameters.

To estimate quantitatively the similarity of the radial PW signals recorded with the EMFi and P(VDF-TrFE) sensors, both concordance correlation coefficient [31] and Pearson's correlation coefficients were calculated for the amplitude-normalized averaged signals. The results are shown in Table 3 for cases in which the four poor-quality measurements are included and excluded. All of the correlation coefficients are greater than 0.97 indicating excellent agreement between the signals of the two sensors.

TABLE 3
THE DISTRIBUTIONS OF THE CORRELATION COEFFICIENTS FOR AVERAGED AMPLITUDE-NORMALIZED INDIVIDUAL PULSE WAVES.

Correlation coefficient	Mean ± standard deviation	Median (inter-quartile range)
Concordance, (outliers included)	0.976 ±0.035	0.987 (0.971…0.994)
Concordance, (outliers excluded)	0.983 ±0.019	0.989 (0.983…0.995)-
Pearson's (outliers included)	0,993±0.007	0.995 (0.990…0.998)
Pearson's (outliers excluded)	0.995±0.005	0.997 (0.990…0.998)

The ratio of the signal amplitudes between the EMFi and P(VDF-TrFE) sensors had inter-subject variations probably caused by the exact placement of the sensor and subsequent

This article has been accepted for publication in a future issue of this journal, but has not been fully edited. Content may change prior to final publication. Citation information: DOI 10.1109/JSEN.2019.2934943, IEEE Sensors Journal

sensitivity changes caused by the multi-directional stress components in the P(VDF-TrFE) sensor, which has non-zero piezoelectric coefficients in orthogonal, longitudinal and shear directions i.e. $d_{33} \cong$ -28 pC/N [35], $d_{31} \cong$ 12 pC/N [32] and $d_{15} \cong$ -30 pC/N, respectively. The $d_{33.f}$ may be therefore either attenuated or amplified depending on the exact mode of deformation (e.g. bending, twisting, stretching) and the dominating non-orthogonal force component. Similar effect was not seen in the signal produced by the EMFi sensor, which is practically sensitive only to the orthogonal loading (f. ex. d_{31} coefficient is two orders of magnitude smaller than d_{33} [33]). The BA-plots with the limits of agreement and scatter plots with reference lines $y=x$ are shown in Fig. 10 for the computed parameters (rAIx, RI, and SI). The BA-ratios, Pearson's correlation, and concordance correlation coefficients are presented in Table 4 for the data shown in Fig. 10. Based on the results, SI has the best agreement between the two sensor outputs. The BA-ratio of rAIx is slightly under the limit for moderate agreement 0.2 and the BA-ratio of RI is slightly over the limit. [29][30]. Despite the inter-subject variations in the agreement, it is shown that careful sensor placement enables recording sufficiently identical PWs with P(VDF-TrFE) and EMFi sensors (Figs 5 and 6) by using a measurement setup originally intended for EMFi sensors, which are not sensitive to shear stress.

One source of uncertainty and differences between the results for the different sensors comes from the feature extraction algorithm: the feature points in a peripheral PW are not always as obvious as in Fig. 5, which is seen especially in Fig. 9a. The feature point extraction algorithm [22] uses a 4th-order derivative analysis as proposed in [40]. The high-order derivative analysis itself is very sensitive to signal noise and the required noise reduction i.e. signal smoothing may slightly distort the resulting PW waveform. This is one reason that may cause different results even though the signal waveform looks similar by visual inspection.

As a summary, it is possible to measure PW signal with both EMFi and P(VDF-TrFE) sensors interchangeably and extract PW-derived features rAIx, RI, and SI if the sensor placement and the signal quality are carefully confirmed during the measurement.

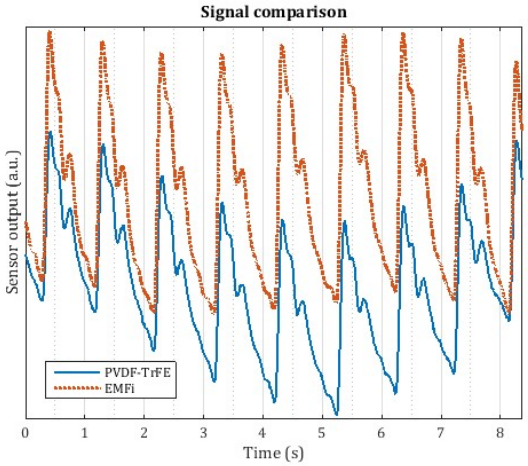

Fig. 8. An example of radial PW signals acquired with the P(VDF-TrFE) (blue continuous line) and EMFi sensors (orange dotted line).

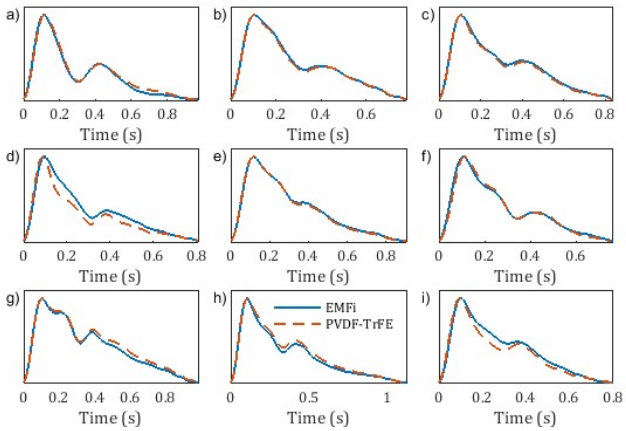

Fig. 9. Examples of amplitude-normalized average pulse waves for nine test subjects. The orange dashed line is for the P(VDF-TrFE) and the blue continuous line for the EMFi sensor.

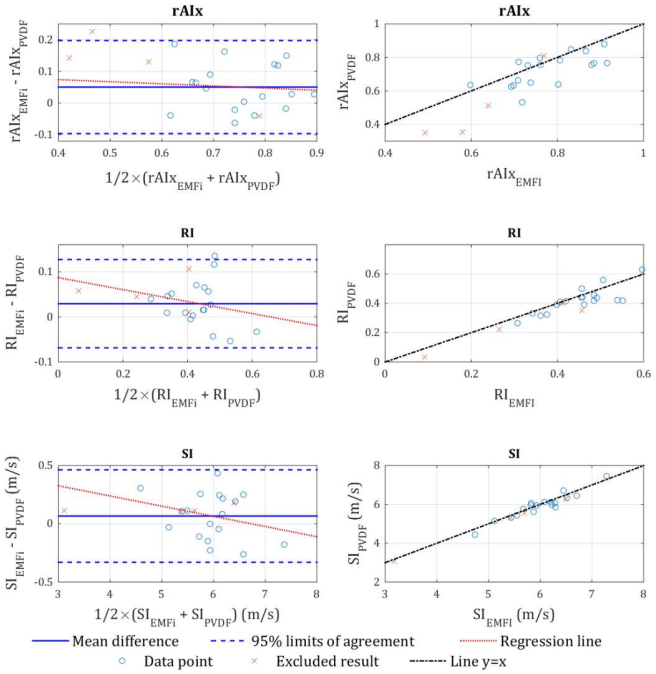

Fig. 10. Bland-Altman plots with the bias (blue continuous line), limits of agreement (blue dashed lines), and regression line (red dotted line) for the differences as well as scatter plots with reference lines $y=x$ (black continuous line).

TABLE 4
BLAND-ALTMAN RATIO (BA-RATIO), CONCORDANCE CORRELATION COEFFICIENTS (CCC) AND PEARSON'S CORRELATION COEFFICIENTS FOR DIFFERENT PARAMETERS.

	BA-ratio	CCC	Pearson's correlation
rAIx	0.195	0.575	0.664
RI	0.225	0.761	0.817
SI	0.067	0.941	0.950

IV. CONCLUSION

We proposed an additive fabrication process for P(VDF-TrFE) based PW-sensors. It was shown that the resulting piezoelectric

properties of the P(VDF-TrFE) compare well with literature values (P_R = 7.3 μC/cm^2, E_c=505 kV/cm, $d_{33.f}$ = (-26.9 ± 2.9) pC/N). The reliability and accuracy of the PW-signal measured with the proposed P(VDF-TrFE) PW-sensor was then evaluated with 22 subjects by extracting clinically relevant indices (rAIx, RI and SI) from the signal and comparing these to indices extracted from concurrently recorded PW-signal which was measured with an EMFi based reference sensor. The comparison of indices was performed using Bland-Altman ratios as well as concordance and Pearson's correlation coefficients. Although the main force component during the PW-measurement is orthogonal to the sensor surface, inaccurate placement of the sensor may cause multi-directional forces, which affect especially the P(VDF-TrFE) PW-sensor due to its higher sensitivity to non-orthogonal force components. However, the results indicate that the two sensors can be used interchangeably as long as the sensor placement is done carefully.

Evaluating the accuracy and reliability of the additively fabricated PW sensors is an important step towards the realization of affordable and unobtrusive on-skin PW-measurement systems suitable for long-term monitoring. As future steps, the additive fabrication of PW-sensor signal acquisition circuitry, communication interface and related energy supply need to be investigated in order to enable the additive fabrication of monolithically integrated PW measurement health patches.

ACKNOWLEDGMENT

The authors wish to thank Dr. Mari Honkanen at Tampere Microscopy Center for the FIBSEM imaging. Authors J.J. and T.S. acknowledge the funding of the Academy of Finland (project number 318203)

REFERENCES

[1] M. F. O'Rourke, and J. Hashimoto. "Mechanical factors in arterial aging: a clinical perspective." *Journal of the American College of Cardiology* vol. 50, no. 1, pp. 1-13, Jul. 2007

[2] M. F. O'Rourke, A. Pauca, X. H. Jiang. "Pulse wave analysis." *Br J Clin Pharmacol*., vol. 51, no. 6, pp. 507-522. Jan. 2001

[3] World Health Organization. "Assessing national capacity for the prevention and control of noncommunicable diseases: report of the 2017 global survey." (2018).

[4] Atcor Medical: *Sphygmocor,* accessed: May. 30. 2019. [Online]. Available: http://atcormedical.com/healthcare-professionals/products/

[5] N. Luo, W. Dai, C. Li, Z. Zhou, L. Lu, C. C. Y. Poon, S.-C. Chen, Y. Zhang and N. Zhao, "Flexible piezoresistive sensor patch enabling ultralow power cuffless blood pressure measurement," *Adv. Funct. Mat.,* vol. 26. no. 8, pp. 1178-1187, Dec. 2015

[6] D.Y. Park, D. J. Joe, D. H. Kim, H. Park, J. H. Han, C. K. Jeong, H. Park, J. G. Park, B. Joung and K. J. Lee, "Self-powered real-time arterial pulse monitoring using ultrathin epidermal piezoelectric sensors", *Adv. Mat.,* vol. 29, no. 37. pp. 1702308, Jul. 2017.

[7] C. Pang, J. H. Koo, A. Nguyen, J. M. Caves, M.-G. Kim, A. Chortos, K. Kim, P. J. Wang, J. B.-H. Tok and Zhenan Bao, "Highly skin-conformable microhairy sensor for pulse signal amplification", *Adv. Mat.* vol. 27, no. 4. pp. 634-640, Jan. 2015

[8] K. Kim, M. Jung, B. Kim, J. Kim, K. Shin., O.-S. Kwon and S. Jeon, "Low-voltage, high-sensitivity and high-reliability bimodal sensor array with fully inkjet-printed flexible conducting electrode for low power consumption electronic skin", *Nano Energy,* vol. 41. pp. 301-307, Nov. 2017

[9] X. Chen, X. Li, J. Shao, N. An, H. Tian, C. Wang, T. Han, L. Wang, B Lu, "High-performance piezoelectric nanogenerators with imprinted P(VDF-TrFE)/BaTiO3 nanocomposite micropillars for self-powered flexible sensors", *Small,* vol. 13, no. 23, p. 1604245, Apr. 2017

[10] X. Chen, H. Tian, X. Li, J. Shao, Y. Ding, N. An, Y. Zhou, "A high performance P(VDF-TrFE) nanogenerator with self-connected and vertically integrated fibers by patterned EHD pulling", *Nanoscale,* vol. 7, no. 27, pp. 11536-11544, May 2015

[11] T. Sekine, R. Sugano, T. Tashiro, J. Sato, Y. Takeda, H. Matsui, D. Kumaki, F. D. D. Santos, A. Miyabo and S. Tokito, "Fully printed wearable vital sensor for human pulse rate monitoring using ferroelectric polymer", *Sci. Rep.,* vol. 8. p. 4442, Mar. 2018

[12] S. Y. Yeo, S. Park, Y. J. Yi, D. H. Kim and J. A. Lim, "Highly sensitive pressure sensors based on printed organic transistors with centro-apically self-organized organic semiconductor microstructures", *ACS Appl. Mat & Interf.,* vol. 9, no. 49, pp. 42996-43003, Nov. 2017

[13] G. Schwartz, B. C.-K. Tee, J. Mei, A. L. Appleton, D. H. Kim, H. Wang and Z. Bao, "Flexible polymer tranasistors with high pressure sensitivity for application in electronic skin and health monitoring", *Nat. Comm.,* vol. 4, pp. 1859, May 2013

[14] S. Gong, W. Schwalb, Y. Wang, Y. Chen, Y. Tang, J. Si, B. Shirinzadeh and W. Cheng, "A wearable and highly sensitive pressure sensor with ultrathin gold nanowires", *Nat. comm.,* vol. 5. pp. 3132, Feb. 2014.

[15] G. Yang, G. Pang, Z. Pang, Y. Gu, M. Mäntysalo, H. Yang, "Non-Invasive Flexible and Stretchable Wearable Sensors with Nano-Based Enhancement for Chronic Disease Care", *IEEE Rev. in Biom. Engin.* vol. 12, pp. 34-71, Dec. 2018

[16] D-H. Kim, N. Lu, R. Ma, Y.-S. Kim, R.-H. Kim, S. Wang, J. Wu, S. M. Won, H. Tao, A. Islam, K. J. Yu, T.-i. Kim, R. Chowdhury, M. Ying, L. Xu, M. Li, H.-J. Chung, H. Keum, M. McCormick, P. Liu, Y.-W. Zhang, F. G. Omenetto, Y. Huang, T. Coleman, J. A. Rogers "Epidermal electronics", *Science,* vol. 333, no. 6022, pp. 838-843, Aug. 2011.

[17] Y. Yamamoto, S. Harada, D. Yamamoto, W. Honda, T. Arie, S. Akita, K. Takei, "Printed multifunctional flexible device with an integrated motion sensor for health care monitoring", *Sci. Adv.,* vol. 2, no. 11, p. 1601473. Nov. 2016

[18] C. M. Lochner, Y. Khan, A. Pierre, A. C. Arias, "All-organic optoelectronic sensor for pulse oximetry", *Nat. Comm.,* vol. 5, p. 5745, Dec. 2014

[19] T. Vuorinen, M.-M. Laurila, R. Mangayil, M. Karp, M. Mäntysalo, "High resolution E-jet printed temperature sensor on artificial skin", *Proc. IFMBE EMBEC NBC*, vol. 64, pp. 839-842, Jun. 2017

[20] M.-M. Laurila, H. Matsui, R. Shiwaku, M. Peltokangas, J. Verho, K. L. Montero, T. Sekine, A. Vehkaoja, N. Oksala, S. Tokito, M. Mäntysalo, "A fully printed ultra-thin charge amplifier for on-skin biosignal measurements", vol. 7, pp. 566-574, May 2019

[21] M. Peltokangas, A. A. Telembeci, J. Verho, V. M. Mattila, P. Romsi, A. Vehkaoja, J. Lekkala and N. Oksala, "Parameters extracted from arterial pulse waves as markers of atherosclerotic changes: performance and repeatability." *IEEE journal of biomedical and health informatics* vol. 22, no. 3, pp. 750-757, May 2018.

[22] M. Peltokangas, Suominen V., D. Vakhitov, J. Verho, J. Korhonen, J. Lekkala, A. Vehkaoja and N. Oksala "The effect of percutaneous transluminal angioplasty of superficial femoral artery on pulse wave features." *Computers in biology and medicine,* vol. 96, no. 1, pp. 274-282, May 2018.

[23] S. Rajala, S. Tuukkanen and J. Halttunen, "Characteristics of piezoelectric polymer film sensors with solution-processable graphene-based electrode materials" *IEEE Sens. Journ.,* vol. 15, no. 6., pp. 3102-3109, Jun. 2015

[24] K. Prume, P. Muralt, F. Calame, T. Schmitz-Kempen, S. Tiedke, "Piezoelectric thin films: evalutation of electrical and electromechanical characteristics for MEMS devices", *IEEE Trans. on Ultr, Ferr. and Freq. Contr.,* vol. 54, no. 1, Jan. 2007

[25] M. Peltokangas, A. Vehkaoja, J. Verho, M. Huotari, J. Röning and J. Lekkala, "Monitoring arterial pulse waves with synchronous body sensor network", *IEEE Journ. of Biomed. and Health Inf.,* vol. 18, no. 6, pp. 1781-1787, Nov. 2014

[26] K. Kohara, Y Tabara, A. Oshiumi, Y. Miyawaki, T. Kobayashi and T. Miki, "Radial augmentation index: a useful and easily obtainable parameter for vascular aging", *American Journal of Hypertension,* vol. 18, no. S1, pp. 11S-14S, Jan. 2005

[27] S. C. Millasseau, J. M. Ritter, K. Takazawa and P. J. Chowienczyk, "Contour analysis of the photoplethysmographic pulse measured at the finger." *Journal of hypertension* vol. 24, no. 8, pp. 1449-1456, 2006

[28] J. M. Bland, D. G. Altman, "Statistical methods for assessing agreement between two methods of clinical measurement" *Lancet,* vol. 327, no. 8476 pp. 307–310, Feb. 1986

[29] J.-S. Wong, W.-A. Lu, K.-T. Wu, M. Liu, G.-Y. Chen and C.-D. Kuo, "A comparative study of pulse rate variability and heart rate variability in healthy subjects." *Journal of clinical monitoring and computing* vol. 26, no.2, pp. 107-114, Apr. 2012

[30] S. W. Weinschenk, R. D. Beise and J Lorenz, "Heart rate variability (HRV) in deep breathing tests and 5-min short-term recordings: agreement of ear photoplethysmography with ECG measurements, in 343 subjects." *European journal of applied physiology* vol. 116, no. 8, pp. 1527-1535, Aug. 2016

[31] I. Lawrence and K. Lin. "A concordance correlation coefficient to evaluate reproducibility." *Biometrics*, vol. 45, no. 1, pp. 255-268, March 1989

[32] C. Ribeiro, C. M. Costa, D. M. Correia, J. Nuner-Pereira, J. Oliveira, P. Martins, R. Gongalves, V. F. Cardoso, S. Lanceros-Mendez, "Electroactive poly(vinylidene fluoride)-based structures for advanced applications", *Nature Protocols,* vol. 13, no. 4, pp. 681-704, March 2018

[33] G. S. Neugschwandtner, R. Schwödiauer, S. Bauer-Gogonea, S. Bauer, M. Paajanen and J. Lekkala, "Piezo- and pyroelectricity of a polymer-foam space-charge electret", *Journ. of Appl. Phys.,* vol. 89. no. 8, pp. 4503-4511, Apr. 2001

[34] D. Damjanovic, "Chapter 4: Hysteresis in piezoelectric and ferroelectric materials," in The Science of Hysteresis vol. 3, Elsevier, 2005. pp. 431-448

[35] Piezotech Arkema Group, *TDS Piezotech FC ink P datasheet,* accessed Jan. 4. 2019. [Online]. Available: https://www.piezotech.eu/en/Technical-center/Documentation/df

[36] T. Furukawa, "Structure and functional properties of ferroelectric polymers", *Advances in Colloid and Interface Sciences,* vol. 71-72, pp. 183-208, Sept. 1997

[37] Y. Pu, J. Zhu, X. Zhu, Y. Luo, M. Wang, X. Li, J. Liu, J. Zhu and D. Xiao, "Double hysteresis loop induced by defect dipoles in ferroelectric $Pb(Zr_{0.8}Ti_{0.2})O_3$ thin films," *Journ. of appl. phys.,* vol 109, pp. 044102, Feb. 2011

[38] J. J. Lee and S. B. Desu, "The shifting of P-E hysteresis loop by the asymmetric contacts on ferroelectric PZT thin films", *Ferroelectr. Lett. Sect.,* vol. 20, pp. 27-34, Aug. 2006

[39] S. Rajala, M. Schouten, G. Krijnen and S. Tuukkanen, "High bending-mode sensitivity of printed piezoelectric poly(vinylidenefluoride-co-trifluoroethylene) sensors", *ACS Omega,* vol. 3., no. 7, pp. 8067-8073, Jul. 2018

[40] K. Takazawa, N. Tanaka, K. Takeda, F. Kurosu and C. Ibukiyama, "Underestimation of vasodilator effects of nitroglycerin by upper limb blood pressure." *Hypertension*, vol. *26*, no.3, pp. 520-523, 1995

Mika-Matti Laurila received his M.Sc. in electrical engineering from Tampere University of Technology, Finland in 2015. He is currently working towards his Ph.D. at the Printable Electronics Research Group at Tampere University. His research interests are related to the applications of inkjet technology in electronics packaging and fabrication of printed piezoelectric sensors for biosignal monitoring

Mikko Peltokangas received his received his M.Sc. degree in biomedical engineering from Tampere University of Technology, Finland in 2013. He is currently working towards his Ph.D. at the Sensor Technology and Biomeasurements group, Faculty of Medicine and Health Technology, Tampere University. His research interests are related to the non-invasive physiological measurements and analysis of physiological signals.

Karem Lozano Montero received her B.Sc. in electronic systems engineering from Polytechnic University of Catalonia, Barcelona, Spain in 2015. She is currently pursuing her M.Sc. in electrical engineering at Tampere University. She is a research assitant at the Printable Electronics research group at Tampere University. Her research focuses on printed pressure sensors for electronic skin applications.

Tuomo Siponkoski received his M.Sc. degree in electrical engineering from the University of Oulu, Finland in 2011. He is currently working towards his Ph.D. in the field of dielectric and piezoelectric materials at the Microelectronics Research Unit, Faculty of Information Technology and Electrical Engineering, University of Oulu. His research interests include printed electronics, materials characterization, sensors, ferroelectrics, piezoelectrics and ultra-low temperature materials.

Jari Juuti received his M.Sc. and D.Sc. degrees in mechanical and electrical engineering from the University of Oulu, Finland, in 2000 and 2006, respectively. He was appointed as Docent/Adjunct professor of "Functional Materials their Components and Applications" at the university in 2009. Currently he is Senior Research Fellow of the University of Oulu and has participated/supervised >30 research projects funded by domestic/international funding agencies and industry. He is author/co-author of >90 refereed scientific journal publications, ~20 conference publications, 3 book chapters and 5 patents/patent applications. His research interests include piezoelectric materials, functional composites, actuators, motors and energy harvesters for micromechanical, high frequency and printed electronics applications.

Sampo Tuukkanen received his P.hD. in applied physics from the Department of Physics, University of Jyväskylä, Jyväskylä, Finland, in 2006. He is currently holding an Associate Professor (tenure track) position at Tampere University, Tampere, Finland. His research interests are related to biomeasurements and bio-based devices. He has authored 48 international peer-reviewed publications, and has an h-index of 18 (Google Scholar).

Niku Oksala received his MD and PhD degrees in medicine and experimental surgery from the University of Eastern Finland in 2000 and 2003, respectively and his DSc(med) degree in molecular biology from Tampere University in 2009. From 2007 he was a consultant vascular surgeon and clinical teacher and from 2014 an associate professor of surgery being tenured full professor in early 2018. He is currently Professor of Vascular Surgery at Tampere University and chief Vascular Surgeon at Tampere University Hospital. He has authored over 150 international journal articles. His current research interests include biomedical sensor technology, clinical research and molecular biology of atherosclerosis. He serves as a board member of Instrumentarium Science Foundation and Finnish Cardiovascular Research Center, Tampere, Finland.

Antti Vehkaoja received his D.Sc. (Tech.) degree in automation science and engineering from Tampere University of Technology, Tampere, Finland in 2015. He has authored more than 70 scientific articles. He is currently an assistant professor (tenure tract) of Sensor technology and biomeasurements at Tampere University. His research interests include development of embedded measurement technologies for physiological monitoring and related signal processing and data analysis methods with a focus on the assessment of vascular condition.

Matti Mäntysalo received his M.Sc. and D.Sc. (Tech.) degrees in electrical engineering from Tampere University of Technology, Tampere, Finland, in 2004 and 2008, respectively. From 2011 to 2012, he was a Visiting Scientist with the iPack Vinn Excellence Center, School of Information and Communication Technology, KTH Royal Institute of Technology, Stockholm, Sweden. He has authored over 100 international journals and conference articles. He is currently Professor of electronics materials and manufacturing with the Tampere University, His current research interests include printed electronics materials, fabrication processes, stretchable electronics, and especially integration of printed electronics with silicon-based technology (hybrid systems). Prof. Mäntysalo was a recipient of the Academy Research Fellow Grant from the Academy of Finland. He has served on the IEEE CMPT, the IEC TC119 Printed Electronics Standardization, and the Organic Electronics Association.